BIOCHEMISTRY
including biophysical chemistry & molecular biology

Article

pubs.acs.org/biochemistry

ArsH from the Cyanobacterium *Synechocystis* sp. PCC 6803 Is an Efficient NADPH-Dependent Quinone Reductase

Manuel Hervás, Luis López-Maury, Pilar León, Ana M. Sánchez-Riego, Francisco J. Florencio, and José A. Navarro*

Instituto de Bioquímica Vegetal y Fotosíntesis, CSIC and Universidad de Sevilla, cicCartuja, Américo Vespucio 49, 41092 Seville, Spain

Supporting Information

ABSTRACT: The cyanobacterium *Synechocystis* sp. PCC 6803 possesses an arsenic resistance operon that encodes, among others, an ArsH protein. ArsH is a flavin mononucleotide (FMN)-containing protein of unknown function and a member of the family of NADPH-dependent FMN reductases. The nature of its final electron acceptor and the role of ArsH in the resistance to arsenic remained to be clarified. Here we have expressed and purified *Synechocystis* ArsH and conducted an intensive biochemical study. We present kinetic evidence supporting a quinone reductase activity for ArsH, with a preference for quinones with hydrophobic substituents. By using steady-state activity measurements, as well as stopped-flow and laser-flash photolysis kinetic analyses, it has been possible to establish the mechanism of the process and estimate the values of the kinetic constants. Although the enzyme is able to stabilize the anionic semiquinone form of the FMN, reduction of quinones involves the hydroquinone form of the flavin cofactor, and the enzymatic reaction occurs through a ping-pong-type mechanism. ArsH is able to catalyze one-electron reactions (oxygen and cytochrome *c* reduction), involving the FMN semiquinone form, but with lower efficiency. In addition, *arsH* mutants are sensitive to the oxidizing agent menadione, suggesting that ArsH plays a role in the response to oxidative stress caused by arsenite.

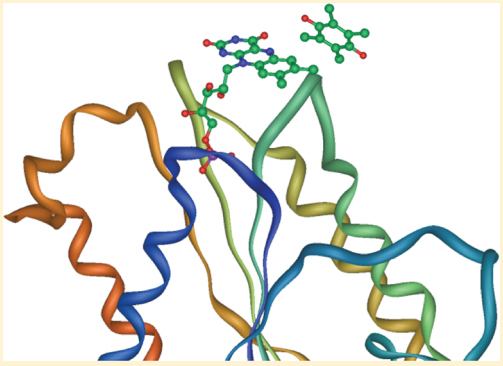

NAD(P)H-dependent flavoproteins, acting as redox enzymes, play different roles in many cellular processes by transferring electrons to a protein substrate or another electron acceptor, as quinones or dithiols. These enzymes are thus involved in essential bioenergetic processes, biochemical degradations, and biosynthesis and detoxification reactions.[1]

One of these detoxification processes involves arsenic, a toxic metalloid generated from both man-made and natural sources[2,3] that can exist in the arsenate (As^{V}) and arsenite (As^{III}) oxyanion forms. Microorganisms have developed arsenic resistance mechanisms, which involve specific arsenic resistance *ars* genes.[4−6] Bacterial *ars* operons usually contain at least three proteins: (i) ArsR, a repressor protein that regulates the basal level of Ars protein expression, (ii) ArsC, an arsenate reductase to support arsenic redox detoxification, and (iii) ArsB, an arsenite membrane transport protein.[4,5,7] In some cases, together with these or other proteins, an ArsH protein of unknown function is also part of the *ars* operon.[6,8−10]

The cyanobacterium *Synechocystis* sp. PCC 6803 (hereafter *Synechocystis*) contains an arsenic and antimony resistance operon that combines elements from Gram-negative and Gram-positive species.[6,11] In addition to a DNA-binding site for the ArsR repressor, the *ars* operon of *Synechocystis* contains *arsB* and *arsC* genes, as well as the gene encoding ArsH. One of the most intriguing questions about the arsenical resistance mechanisms is the biochemical role of the ArsH protein.[6,12]

ArsH proteins are widely distributed in bacteria. Whereas it is clear that the protein has no arsenate reductase activity, in some cases ArsH confers resistance to arsenicals.[13,14] However, in *Synechocystis*, ArsH does not confer arsenic resistance.[6] Crystal structures of the apoprotein of bacterial ArsH are available.[10,15] From these structures, as well as from kinetic studies and protein sequence analysis, it is well established that ArsHs are FMN-containing members of the family of NADPH-dependent FMN reductases. ArsH crystallizes as tetramer units, forming a dimer of dimers; each monomer is a global $\alpha\beta$ protein with a flavodoxin-like single-core domain architecture, and N- and C-terminal extensions forming a small domain involved in subunit interactions.[10,15]

It is clear that the catalytic cycle of ArsH consists of the acceptance of two electrons from NADPH to reduce the flavin cofactor (reductive half-reaction) and the transfer of these electrons to an acceptor (oxidative half-reaction).[10,15] However, although ArsH has been proposed to act as a FMN-reductase,[10] an azoreductase, or a H_2O_2-producing enzyme involved in arsenate detoxification,[15] the nature of the final electron acceptor (or acceptors) and the role of ArsH in the resistance to arsenic remain to be clarified.

Received: December 21, 2011
Revised: January 17, 2012
Published: January 23, 2012

dx.doi.org/10.1021/bi201904p | *Biochemistry* 2012, 51, 1178−1187

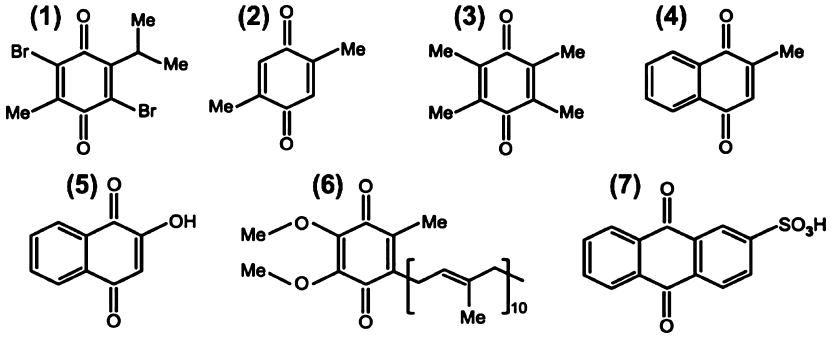

Figure 1. Chemical structure of the quinones used in this study. Quinones are numbered as in Table 1: dibromothymoquinone (DBMIB) (**1**), 2,5-dimethyl-*p*-benzoquinone (dimethyl-*p*-BQ) (**2**), duroquinone (**3**), menadione (**4**), 2-hydroxy-1,4-naphthoquinone (2-OH-1,4-NQ) (**5**), coenzyme Q_{10} (**6**), and anthraquinone-2-sulfonate (AQS) (**7**).

Here we have expressed and purified *Synechocystis* ArsH and conducted an intensive biochemical study. We present kinetic evidence supporting a quinone-reductase role for ArsH. In addition, *arsH* mutants are sensitive to the oxidizing agent menadione, suggesting that ArsH has a role in the response to oxidative stress caused by arsenite.

EXPERIMENTAL PROCEDURES

Biological Material. For the cloning, expression, and purification of ArsH, the *arsH* ORF was amplified by polymerase chain reaction using ARSH3 (covering the starting codon of *arsH* and introducing a *Nde*I restriction site) and ARSC3 (which introduces a *Sal*I restriction site after the stop codon of *arsC*) oligonucleotides, digested with *Nde*I and *Sal*I, and cloned into pET28 (Novagen) digested with the same enzymes, generating pARSHHIS. The plasmid expresses ArsH protein fused to six histidines and a thrombin cleavage site at its N-terminus. *Escherichia coli* BL21(DE3) cells transformed with pARSHHIS were used for expression of the cloned gene. The cells were grown at 150 rpm and 37 °C in 2.5 L (in 5 L Erlenmeyer flasks) of standard Luria-Bertani (LB) medium, supplemented with 100 μg/mL kanamycin, until an OD_{580} of ≈0.5 was reached. Protein expression was induced by adding 1 mM IPTG, and cells were then maintained at 30 °C until an OD_{580} of ≈1 was reached. Cells were collected by centrifugation and the pellets resuspended in 50 mM phosphate buffer (pH 8.0) supplemented with 0.5 M NaCl, 1 mM PMSF, and 1 unit of DNase. Cells were broken by being passed three times through a French press (13000 psi), and the homogenates were cleared by ultracentrifugation. ArsH was purified by fast-performance liquid chromatography (FPLC) using 5 mL HiTrap Chelating HP columns (GE Healthcare), loaded with nickel and prepared as described by the manufacturer. The recombinant protein was eluted with a 0.04 to 0.5 M imidazole gradient in 50 mM phosphate/0.5 M NaCl buffer (pH 8.0). ArsH fractions were dialyzed against 5 mM phosphate buffer (pH 7.5) supplemented with 10 mM imidazole, 5 mM NaCl, and 0.03% β-dodecyl maltoside, concentrated by ultrafiltration (up to 0.7 mM protein), and stored at −80 °C until they were used.

The *arsH* deletion (SARSH) and *arsR* deletion (SARSR) strains were constructed as previously described.[6] Analysis of the growth of both deletion strains as compared with that of the wild type (WT) was conducted in BG11C solid medium plates, supplemented with 10 μM menadione, with or without 1 mM arsenite. The plates were maintained at 30 °C for 5−7 days to visualize the differences in growth.

Analytical Methods. The purity and molecular mass of ArsH were checked by sodium dodecyl sulfate−polyacrylamide gel electrophoresis (SDS−PAGE). The native molecular weight was determined by gel filtration using an analytical Superose 6 HR 10/30 column (GE Healthcare) connected to an FPLC instrument. The apparent molecular mass was estimated by comparison with Bio-Rad standards (catalog no. 151-1901).

Protein concentrations were determined spectrophotometrically using a molar absorption coefficient of 11.4 mM^{-1} cm^{-1} at 453 nm, as here calculated using the method described by Mayhew and Massey.[16] An A_{275}/A_{453} ratio of 5.1 was obtained at the end of the purification process. The flavin cofactor associated with the protein was identified by high-performance liquid chromatography (HPLC) as described by Light et al.,[17] using FAD and FMN solutions as standards.

Redox titrations of 20−25 μM ArsH samples were performed in a diode array spectrometer (Hewlett-Packard 8452A) in 50 mM Tris-HCl (pH 7.5) under anaerobic conditions by previous sample bubbling with argon. NADPH titrations were performed by adding fixed amounts of the nucleotide (0.5−1 μM) until no additional absorbance changes were observed, which allowed us to estimate the NADPH:ArsH ratio needed to accomplish full protein reduction. The ArsH redox potential was determined by phototitration, as described previously.[18] For oxidative titrations, small amounts of oxygen were introduced into the previously reduced sample. Absorbance changes at 453 nm were used to estimate the relative amounts of reduced and oxidized protein. Benzyl-viologen, 2-hydroxy-1,4-naphthoquinone, and anthraquinone-2-sulfonate (5 μM each) were used as redox mediators.

Steady-State Enzymatic Assays. ArsH-catalyzed arsenate reduction activity was assayed as NADPH consumption in the presence of sodium arsenate, ArsH being totally inactive. The NADPH-dependent quinone reductase activity of ArsH was determined spectrophotometrically by following NADPH oxidation at 340 nm. All measurements were taken anaerobically at 25 °C in 50 mM Hepes (pH 8.0) under magnetic-bar stirring. To calculate the ArsH K_m for quinone, the catalytic constant (k_{cat}), and the catalytic efficiency ($E_{cat} = k_{cat}/K_m$) values for each quinone, the standard reaction mixture contained 110 μM NADPH, 4−20 nM ArsH, and different concentrations of the corresponding quinone. The following commercial-grade quinones were used: dibromothymoquinone (DBMIB), 2,5-dimethyl-*p*-benzoquinone (dimethyl-*p*-BQ), duroquinone, menadione, 2-hydroxy-1,4-naphthoquinone (2-OH-1,4-NQ), coenzyme Q_{10}, and anthraquinone-2-sulfonate (AQS) (Figure 1). The kinetic parameters were obtained from

dx.doi.org/10.1021/bi201904p | *Biochemistry* 2012, 51, 1178−1187

double-reciprocal plots of the initial velocity of NADPH consumption versus quinone concentration. Calculation of the ArsH K_m for NADPH was achieved by using either 70 μM DCPIP or 150 μM 2-OH-1,4-NQ as the electron acceptor, 20 nM ArsH, and different concentrations of NADPH; alternatively, 150 μM $NADP^+$ was also added to the initial solutions for the analysis of the inhibitory effect of the oxidized nucleotide. Methyl-red reduction by ArsH (azoreductase activity)[19,20] was followed at 430 nm (dye decoloration) in 0.1 M Hepes buffer (pH 8.0) in the presence of 110 μM NADPH and 0.2 μM ArsH at different dye concentrations. Horse oxidized cytochrome *c* (*Cc*) (Sigma) reduction, used as a reporter of one-electron reductions,[21] was followed at 550 nm in 50 mM Hepes buffer (pH 8.0) in solutions containing 200 μM NADPH, 4 nM ArsH, 100 μM quinones, and 10 μM *Cc*. The cytochrome was previously oxidized by potassium ferricyanide and intensively washed via ultrafiltration to remove the oxidant. Hydrogen peroxide generation was measured in aerobic solutions containing 0.5 mM NADPH, 0.2 μM ArsH, and 50 μM quinones, using the peroxidase/*o*-dianisidine assay as described previously.[22]

Transient Kinetic Methods. Stopped-flow experiments were conducted in 20 mM phosphate buffer (pH 7.5) at 10 °C under anaerobic conditions, using a μSFM-20 device fitted with a TC-50/10 cuvette (5 mm path length) and coupled to a MOS-450 spectrophotometer (Bio-Logic). Reduction of ArsH by either NADPH or NADH was followed at 453 and 560 nm by mixing 200 μL solutions of 10 μM $ArsH_{OX}$ with small volumes of concentrated nucleotide solutions (1−4 mM), in the presence of 20 mM glucose and 5 units/mL glucose-oxidase and catalase. For quinone reduction experiments, the ArsH hydroquinone form ($ArsH_{HQ}$) was generated in situ in the stopped-flow syringe by light irradiation in the presence of 0.5 μM 5-deazariboflavin (dRf) and 5 mM EDTA until the sample decoloration indicated ~100% $ArsH_{HQ}$ generation.[18,23] Solutions (200 μL) of 7 μM $ArsH_{HQ}$ were mixed with small volumes of concentrated quinone solutions (≥100 μM), and evolution of the processes was followed at 453 nm. In all cases, the observed rate constants (k_{obs}) were calculated by fitting to mono- or multiexponential processes by using the Bio-Kine32 software package from Bio-Logic. Estimated errors in the determined values were ±5%.

Laser-flash experiments were performed anaerobically at room temperature in a 1 cm path-length cuvette, using dRf as a photosensitizer in the presence or absence of an excess of methyl-viologen (MV) as previously described.[24,25] The redox changes of ArsH were monitored at 460 nm.

The standard reaction mixture contained, in a final volume of 1.5 mL, 25 mM sodium phosphate buffer (pH 7.5), 5 mM EDTA, 100 μM dRf, 60 μM $ArsH_{OX}$, and quinones at varying concentrations, in the absence or presence of 1 mM MV. All experiments were performed under pseudo-first-order conditions, for which the amount of acceptor (oxidized quinone) was maintained well in excess over the amount of the generated reduced ArsH. Each kinetic trace was the average of six to eight measurements. Kinetic analyses were performed according to the reaction mechanisms previously proposed.[26] Estimated errors in the determined values were ±10%.

Structural Model of ArsH Reconstituted with FMN. The in silico *Synechocystis* ArsH model was generated by the Phyre web server (http://www.sbg.bio.ic.ac.uk/~phyre/) using Phyre-1, with the crystal structure of the apo-ArsH protein from *Sinorhizobium meliloti* [Protein Data Bank (PDB) entry 2Q62, 75% identical (see Figure S1 of the Supporting Information)] as the best template.[15] The FMN coordinates from T1501, a FMN reductase from *Pseudomonas aeruginosa* (PDB entry 1X77),[27] were then introduced into the model. Finally, protein energy minimization was conducted with Swiss-Pdb Viewer in two steps, first selecting residues in the vicinity of FMN and then the full protein, following in both cases 1000 steps of steepest descent (SD) and 2000 steps of conjugate gradient (CG).

RESULTS

Expression, Purification, and Characterization of the ArsH Protein from *Synechocystis*. Cloning of the *arsH* gene into an IPTG-inducible expression vector led to the expression and purification of the 226-residue protein with a mass of 25.9 kDa, as deduced from its amino acid sequence and SDS−PAGE. However, the native molecular mass determined by size-exclusion chromatography (108 kDa) is compatible with a tetrameric form of the enzyme (not shown). Purified ArsH exhibits a typical flavoprotein absorption spectrum, with major peaks at 453, 375, and 275 nm (Figure 2) resulting from the binding of a FMN cofactor, as determined by HPLC, in a 1:1 stochiometry (not shown).

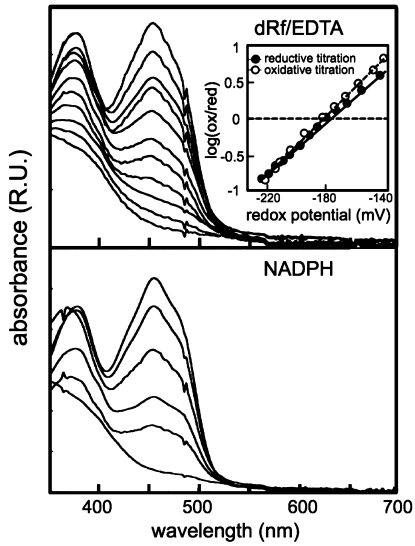

Figure 2. ArsH (20 μM) photoreduction (top) by short pulses of white light in the presence of 1 μM dRf and 5 mM EDTA. The inset shows Nernst plots for the reductive (●) and oxidative (○) ArsH redox titrations. Representative spectra (bottom) for progressive reduction of a 25 μM ArsH sample by adding repeated fixed amounts (0.5−1 μM) of NADPH. The top spectrum is the initial spectrum without NADPH, and the bottom spectrum is that with 28 μM NADPH. Other experimental conditions were as described in Experimental Procedures.

The amino acid sequence of *Synechocystis* ArsH is highly homologous to those of other cyanobacterial ArsHs, as well as to those of the ArsH proteins from *S. meliloti* (75% identical) and *Shigella flexneri* (70% identical) (see Figure S1 of the Supporting Information), for which crystal structures of homotetrameric apo forms are already available.[10,15] As found in other ArsH proteins, *Synechocystis* ArsH exhibits the typical binding motif for NADPH [(V/T)(S/T)GGSQS].[10]

ArsH Reductive Reactions. ArsH samples were subjected to one- and two-electron reduction under steady-state

anaerobic conditions (Figure 2). Similar flavin cofactor spectra are observed when ArsH is gradually reduced, either with NADPH (two-electron donor) or with the dRf/EDTA system (one-electron donor). In both cases, final spectra are characteristic of the fully reduced $ArsH_{HQ}$ species, as previously described for similar enzymes.[28] However, whereas reduction of ArsH by NADPH can take place directly without the occurrence of $ArsH_{SQ}$, the spectra observed with reduction by dRfH can also be explained by the intermediate formation of the anionic semiquinone form of the FMN cofactor in the course of the titration.[29] This species cannot be easily detected because of the lack of absorbance in the 500−700 nm range typical of neutral semiquinones,[29] which will be stated below when discussing the laser-flash experiments. In the case of NADPH reduction, a 1:1 NADPH:ArsH stochiometry is enough to accomplish protein reduction.

From the absorbance spectra shown in the top panel of Figure 2, and with simultaneous measurement of the ambient redox potential in the cuvette, redox titrations could be conducted. Both reductive and oxidative ArsH redox titration data fit well to a single sigmoidal curve (not shown), thus suggesting that the redox potential values for the $ArsH_{OX}$/$ArsH_{SQ}$ and $ArsH_{SQ}$/$ArsH_{HQ}$ couples are relatively similar. A midpoint redox potential of −181 ± 2 mV, at pH 7.5, was calculated from the linear Nernst plots (Figure 2, top inset), which corresponds to the overall potential of the $ArsH_{OX}$/$ArsH_{HQ}$ couple. As a comparison, a midpoint redox potential of −0.202 V for free FMN was measured for the overall two-electron reduction (not shown), indicating that the influence of the protein appears scarce in modulating this value in ArsH.

Homologous ArsH proteins have been previously described as NADPH-dependent FMN reductases, whereas very weak or any protein reduction is achieved in the presence of NADH.[10,15] *Synechocystis* ArsH can be reduced by NAD(P)H, although with a clear preference for NADPH, as measured by stopped-flow spectrophotometry (Figure 3). NADPH-dependent ArsH reduction occurs in three phases (Figure 3, top). The first and faster step is basically complete in the dead time of the instrument (~10 ms; $k_{obs} \geq 200\ s^{-1}$) and can be monitored as both an absorbance decrease at 453 nm and a small increase at 560 nm, the latter showing an amplitude ≈10−15 times smaller than that of the absorbance change at 453 nm (Figure 3, top). Whereas this fast phase accounts for ~10−15% of the total change observed at 453 nm, the next step represents the predominant absorbance change at this wavelength, with a constant absolute amplitude that accounts for ≈65% of the total absorbance decrease, and showing a hyperbolic increase in the k_{obs} with NADPH concentration until it reaches a saturation plateau (Figure 3, bottom). Equivalent kinetics for this intermediate phase were observed at 560 nm, but as the disappearance of the initial increase arising from the first phase (Figure 3, top inset). Finally, a slower step is observed as an additional decrease in absorbance at 453 nm (Figure 3, top), the amplitude of this phase decreasing with increasing NADPH concentration (Figure 3, top). Thus, the proportion of this slowest phase decreases from ~30 to 16% of the changes at 453 nm as the concentration of NADPH increases from 22 to 130 μM (not shown). The corresponding observed rate constants seem to be independent of NADPH concentration (not shown), with an apparent value (k_3') of 2 s^{-1} (Table 1).

Equivalent phases for reduction of flavoproteins by NAD(P)H have been previously described.[30−34] Thus, although our equipment does not offer a full spectral range transient

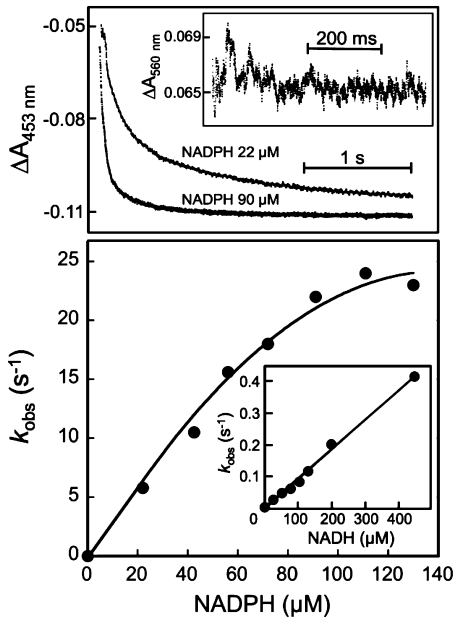

Figure 3. Transient kinetics (top) of ArsH reduction at two different concentrations of NADPH as observed by stopped-flow analysis at 453 nm. Kinetic traces could be adjusted to three-exponential fits. The top inset shows ArsH reduction at 90 μM NADPH measured at 560 nm. Dependence of the observed rate constants (k_{obs}) (bottom) of the intermediate phase of ArsH reduction on NADPH concentration. The bottom inset shows the dependence of k_{obs} for ArsH reduction on NADH concentration. Experiments were conducted in 20 mM phosphate buffer (pH 7.5) at 10 °C under anaerobic conditions. ArsH reduction was followed by mixing 200 μL solutions of 10 μM ArsH with small volumes of concentrated nucleotide solutions (1−4 mM). Solid lines represent theoretical fits according to the reaction mechanisms previously proposed.[26] Other experimental conditions were as described in Experimental Procedures.

measurement, prior stopped-flow experiments with other flavoproteins have reported very rapid formation of NADPH:-flavin charge-transfer complexes ($k_{obs} \approx 500\ s^{-1}$) with absorbance bands in the 500−800 nm region that fit with the absorbance changes associated with the fast initial phase described in this work.[30−34] The second phase involves the decay of the NADPH:flavin charge-transfer complex and the reduction of the flavin cofactor on a time scale of hundreds of milliseconds to form the E_{red}:$NADP^+$ species.[30−34] From the NADPH concentration dependence plot shown in Figure 3 (bottom), it is possible to estimate minimal values for both the association constant ($K_A = 1.7 \times 10^4\ M^{-1}$; $K_D = 59\ \mu M$) and the apparent electron-transfer rate constant ($k_2' = 25\ s^{-1}$) (Table 1) for this process. With regard to the third slowest phase, in some multidomain flavoenzymes, as is the two-cofactor FAD-disulfide thioredoxin-reductase protein, it has been proposed to represent either enzyme reduction by a second NADPH equivalent or a rate-limiting structural rearrangement of the FAD and NADPH domains.[35] However, such explanations are unlikely in the case of the monodomain ArsH protein. Alternatively, the third phase can be assumed to represent the formation of a reduced-flavin:$NADP^+$ charge-transfer species at low NADPH concentrations.[30−34] Finally, ArsH reacts very inefficiently with NADH (Figure 3, bottom inset), and the linear dependence of k_{obs} values on nucleotide concentration allows the calculation of a second-order reaction rate for this process [$k_2 = 920\ M^{-1}\ s^{-1}$ (Table 1)].

dx.doi.org/10.1021/bi201904p | *Biochemistry* 2012, 51, 1178−1187

Table 1. Kinetic Parameters for Reduction and Oxidation of ArsH by Different Substrates

electron donor	k_2 (M^{-1} s^{-1})[a]	K_A (M^{-1})[b]	k_2' (s^{-1})[c]	k_3' (s^{-1})[d]	K_m (μM)
deazariboflavin	1.7×10^8(a)				
methyl-viologen	2.9×10^8(a)				
NADPH		1.7×10^4	25.0	2.0	31.5
NADH	920 (b)				
electron acceptor	k_{SQ}' (s^{-1})[e]	k_{HQ}' (s^{-1})[f]	K_m (μM)	k_{cat} (s^{-1})	E_{cat} (M^{-1} s^{-1})
DBMIB (**1**)	130[h]	nd[i]	1.2	35.0	2.9×10^7
dimethyl-*p*-BQ (**2**)	900[h]	nd[i]	1.3	36.7	2.8×10^7
duroquinone (**3**)	29.0	nd[i]	2.8	25.0	8.9×10^6
menadione (**4**)	45.0	nd[i]	5.7	26.0	4.6×10^6
2-OH-1,4-NQ (**5**)	8.0	48.0	23.7	11.0	4.6×10^5
coenzyme Q_{10} (**6**)	22.0	nd[i]	11.9	5.0	4.2×10^5
AQS (**7**)	nr[k]	2.3	34.5	9.4	2.7×10^5
methyl-red[g]			600	0.4	6.6×10^2

[a] k_2, second-order rate constant for ArsH reduction determined by laser spectroscopy (a) or stopped-flow analysis (b). [b] K_A, association constant obtained by stopped-flow analysis from the concentration dependence of the observed intermediate phase. [c] k_2', first-order electron-transfer rate constant for ArsH reduction estimated by extrapolating at infinite NADPH concentration the rate constant of the intermediate phase observed by stopped-flow analysis. [d] k_3', first-order rate constant for the ArsH–$NADP^+$ rearrangement step estimated by the concentration-independent third phase measured by stopped-flow analysis. [e] k_{SQ}', observed first-order electron-transfer rate constant for oxidation of $ArsH_{SQ}$ by quinones determined by laser spectroscopy. [f] k_{HQ}', observed first-order electron-transfer rate constant for oxidation of $ArsH_{HQ}$ by quinones determined by stopped-flow analysis. [g] Azoreductase activity. [h] k_{obs} at low quinone concentrations. [i] Not detectable because the reaction occurs within the dead time of the stopped-flow experiment. [k] Not reactive on the laser spectroscopy apparatus time scale.

Oxidation of $ArsH_{HQ}$ by Quinones. ArsH from *Synechocystis* is highly homologous to other ArsH proteins and NADPH-dependent FMN reductases. However, a minor but remarkable homology is also found with plant quinone-reductases [~25% identical (see Figure S2 of the Supporting Information)]. Here several quinones have been assayed as acceptors of electrons from the $ArsH_{HQ}$ species reduced either by dRf or NADPH.

Stopped-flow experiments in which $ArsH_{HQ}$ was mixed with different quinones showed that ArsH oxidation occurs within the dead time of the instrument in most cases ($k_{obs} \geq 200$ s^{-1}), as demonstrated by the appearance of the spectrum of $ArsH_{OX}$ at the end of the mixing (not shown). Only when assaying 2-OH-1,4-NQ and AQS were slower kinetics of ArsH oxidation independent of quinone concentration observed (Figure 4), with k_{obs} values (k_{HQ}') of 48.0 and 2.3 s^{-1}, respectively (Table 1).

To further characterize the ArsH quinone-reductase activity, a steady-state enzymatic study was conducted. Figure 5 (top inset) shows as an example the time course of the NADPH-dependent 2-OH-1,4-NQ reduction catalyzed by ArsH, measured as NADPH oxidation at 340 nm. Double-reciprocal plots of the initial velocity of the reaction versus quinone concentration in the presence of different NADPH amounts resulted in parallel lines (Figure 5, top), indicating the occurrence of a ping-pong-type mechanism, in which only after the first substrate (e.g., the nucleotide) is released from the active site can a second substrate (e.g., the quinone) bind and react with the reduced enzyme, thus regenerating the oxidized ArsH form. Double-reciprocal plots for NADPH oxidation as a function of the nucleotide concentration, at saturating amounts of both 2-OH-1,4-NQ and DCPIP, showed linear dependencies (Figure 5, bottom inset), from which it is possible to calculate a similar K_m value of ≈30 μM for NADPH (Table 1). Similar double-reciprocal plots for NADPH oxidation as a function of the concentration of different quinones, at saturating amounts of NADPH, also showed linear dependencies (see Figure 5, top, for 110 μM NADPH) from

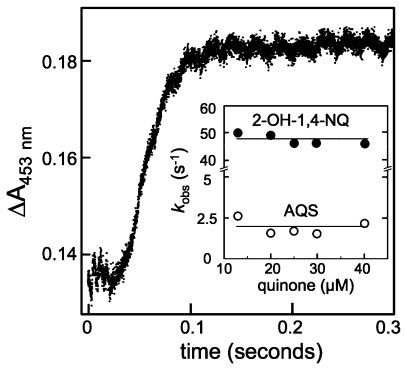

Figure 4. Transient kinetics of $ArsH_{HQ}$ oxidation in the presence of 25 μM 2-OH-1,4-NQ as observed by stopped-flow absorption measurements at 453 nm. The inset shows the dependence of k_{obs} for $ArsH_{HQ}$ oxidation on quinone concentration. $ArsH_{HQ}$ was generated in the stopped-flow syringe by light irradiation in the presence of dRf/EDTA. Solutions (200 μL) of 7 μM $ArsH_{HQ}$ were mixed with small volumes of concentrated quinone solutions. Other experimental conditions were as described in the legend of Figure 3.

which it is possible to make an estimation of the ArsH K_m for the different quinones, as well as the catalytic constants (k_{cat}) and catalytic efficiencies (E_{cat}) of the redox processes (Table 1). Thus, whereas K_m values vary from 1 to 35 μM, E_{cat} spans roughly in a parallel way the range of 10^5–10^7 M^{-1} s^{-1} (Table 1). It is important to note that the kinetic parameters for coenzyme Q_{10} represent only approximate values, as the water insolubility of this quinone impedes experiments conducted at final concentrations of >10 μM.

Flavoenzymes could reduce quinones by one- or two-electron reactions to form the substrate semiquinone or hydroquinone species, respectively; whereas the latter species is relatively stable, the former is able to efficiently reduce one-electron acceptors, such as cytochrome *c* (*Cc*) or oxygen, in the last case involving superoxide ($O_2^{\bullet-}$) formation and further radical deproportionation to generate H_2O_2.[21,36] Thus, *Cc* reduction or H_2O_2 production can be used as a reporter of

dx.doi.org/10.1021/bi201904p | *Biochemistry* 2012, 51, 1178–1187

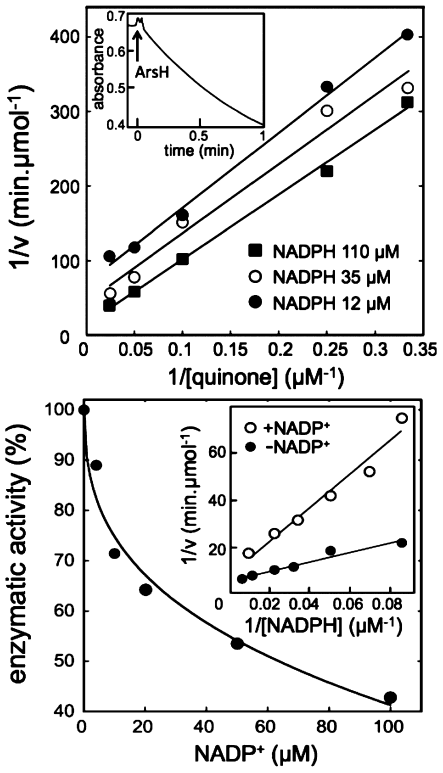

Figure 5. Double-reciprocal plot (top) of the initial velocity (v) of ArsH-catalyzed NADPH oxidation, measured at 340 nm, vs 2-OH-1,4-NQ concentration at different concentrations of NADPH. The top inset shows the time course of NADPH oxidation at 110 μM NADPH and 150 μM 2-OH-1,4-NQ. The arrow indicates the addition of 20 nM ArsH. Effect of $NADP^+$ on the reduction of DCPIP (70 μM) by ArsH (20 nM) (bottom) in the presence of NADPH (50 μM). The enzymatic activity is shown as the percentage of the initial velocity of DCPIP reduction, measured at 600 nm, in the absence of $NADP^+$. The bottom inset shows double-reciprocal plots of the initial velocity (v) of NADPH oxidation by ArsH vs NADPH concentration in the presence of 150 μM 2-OH-1,4-NQ and 20 nM ArsH with or without 150 μM $NADP^+$. Measurements were taken anaerobically at 25 °C in 50 mM Hepes (pH 8.0). Other experimental conditions were as described in Experimental Procedures.

protein-mediated semiquinone production.[21] We have checked the mechanism of ArsH-catalyzed quinone reduction by using different quinones, under anaerobic conditions in the presence of oxidized *Cc*, or under aerobic conditions, both *Cc* and oxygen acting as a "trap" of the generated semiquinone[21] (not shown). Remarkably, NADPH-reduced ArsH is able to reduce *Cc* with a low efficiency in the absence of quinones [≈2 μmol of *Cc* (μmol of ArsH)$^{-1}$ s^{-1} for one-electron transfer, as compared with ≈35 μmol of NADPH (μmol of ArsH)$^{-1}$ s^{-1} for the two-electron-transfer DBMIB reduction]. However, when using DBMIB, dimethyl-*p*-BQ, or duroquinone as the primary substrate for the enzyme, no relevant increases in the rate of *Cc* reduction were observed (not shown). In the same way, quinone-mediated H_2O_2 production under aerobic conditions was negligible (not shown). These results indicate that NADPH-dependent quinone reduction by ArsH predominantly proceeds via two-electron transfer, as in other NADPH-dependent flavoenzymes.[20]

ArsH Alternative Electron Acceptors. ArsH enzymes have been proposed to reduce O_2 to H_2O_2 via superoxide radical generation, as part of a new mechanism for the detoxification of the very toxic arsenite species, involving its oxidation by hydrogen peroxide to form the less toxic arsenate species.[15] *Synechocystis* ArsH can use O_2 as an electron acceptor in the presence of NADPH, but this process is quite inefficient [NADPH decay of ≈0.5 μmol (μmol of ArsH)$^{-1}$ s^{-1} in oxygen-saturated solutions (not shown)].

Quinone reductases are usually able to conduct the reduction of azo bonds and thus present azoreductase activity, perhaps as part of an enzymatic detoxification system.[20] Here we have checked the azoreductase activity of ArsH using the methyl-red dye as an electron acceptor, by measuring the initial velocity of dye decoloration at 430 nm[20] at a saturating NADPH concentration (120 μM). A double-reciprocal plot of the initial velocity versus methyl-red concentration (not shown) allowed the estimation of the ArsH K_m (0.6 mM) for the dye, as well as the k_{cat} (0.4 s^{-1}) and E_{cat} (6.6 × 10^2 M^{-1} s^{-1}) values of the azoreductase activity (Table 1), which proved to be a very inefficient process, as previously reported for other ArsH proteins.[10] Experiments conducted with chromate (40−200 μM) as an alternative electron acceptor[37] rendered also a very residual activity. As previously reported, the enzyme has no arsenate reductase activity (not shown).

ArsH Inhibition. $NADP^+$ can act as a competitive inhibitor for NADPH binding at the active site of an enzyme, which is indeed the case for ArsH from *Synechocystis*. Figure 5 (bottom) shows the decrease in the initial velocity of DCPIP reduction with increasing amounts of $NADP^+$ at a fixed NADPH concentration of 50 μM. This inhibitory effect is better shown by double-reciprocal plots as a function of NADPH concentration in the presence or absence of 150 μM $NADP^+$ (Figure 5, bottom inset). This representation gives two lines intersecting at the same value on the $1/v$ axis, thus indicating a competitive inhibition mechanism with an apparent K_m' value of 82.2 μM in the presence of $NADP^+$. From this value, an inhibition constant (K_i) of 0.1 mM for $NADP^+$ can be estimated.

Dicoumarol, a compound structurally similar to a dimer of menadiones, is a potent competitive inhibitor with respect to nicotinamide coenzymes, particularly in enzymes such as NQO1 quinone-reductases. Dicoumarol concentrations in the submicromolar range are usually enough for total enzyme inhibition.[20] Dicoumarol, however, exerts a much weaker inhibitory effect on ArsH, as concentrations between 8 and 10 μM are required to attain 50% inhibition when using saturating amounts of either DCPIP or 2-OH-1,4-NQ as electron acceptors in the presence of 50 μM NADPH (not shown).

Laser-Flash Spectrophotometry Experiments. All the previous assays presented here are based on the use of NADPH as the electron donor, thus involving the direct generation of the $ArsH_{HQ}$ species. However, as demonstrated with *Cc* and oxygen, $ArsH_{HQ}$ can reduce one-electron acceptors, which generates the flavosemiquinone species. Consequently, the pertinent question of whether the $ArsH_{SQ}$ species is stable enough and thus relevant in reducing quinones arises. By using laser-flash spectroscopy and flavins as redox probes, it is possible to induce one-electron reduction and follow further rapid electron-transfer processes.[23] Figure 6 (top) shows the absorbance changes at different wavelengths associated with ArsH reduction by $dRfH^\bullet$ after the laser flash; the observed decrease in absorbance in the 400−500 nm range, without any significant increase at longer wavelengths, confirms the very rapid formation of the $ArsH_{SQ}$ anionic species [≪1 ms at the

dx.doi.org/10.1021/bi201904p | *Biochemistry* 2012, 51, 1178−1187

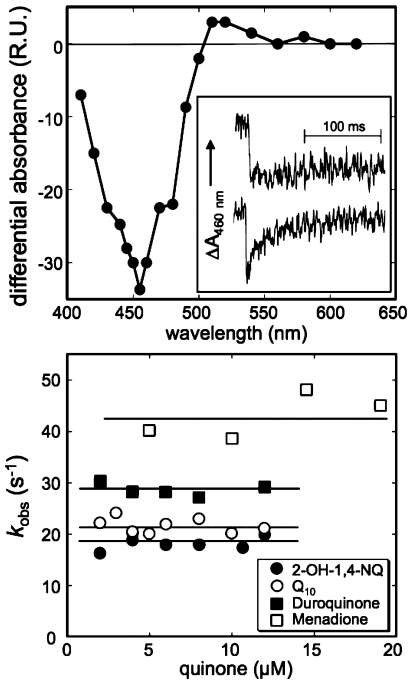

Figure 6. Laser-flash-induced difference spectrum (top) of a solution containing 20 μM ArsH in the presence of 100 μM dRf and 5 mM EDTA. Differential absorbance changes were measured 20 ms after the laser flash. The top inset shows kinetic traces of $ArsH_{SQ}$ generation and decay measured at 460 nm in the absence (top trace) or presence (bottom trace) of 10 μM menadione in a solution containing 60 μM ArsH, 100 μM dRf, 1 mM MV, and 5 mM EDTA. Dependence of k_{obs} for ArsH oxidation on the concentration of different quinones (bottom) as measured by laser-flash spectroscopy. All measurements were taken in 25 mM phosphate buffer (pH 7.5) at 25 °C. Other experimental conditions were as described in Experimental Procedures.

ArsH concentration used in quinone reduction experiments (see below)],[1,29] which is stable on a time scale of hundreds of milliseconds (Figure 6, top inset). Thus, these results indicate that ArsH photoreduction shown in Figure 2 (top) proceeds with the intermediate formation of a stable $ArsH_{SQ}$ anionic species. From the slope of the linear plot of k_{obs} versus ArsH concentration (not shown), a k_2 of 1.7×10^8 M^{-1} s^{-1} for ArsH reduction was obtained (Table 1). The same experiment was conducted in the presence of MV as a redox intermediate between dRf and ArsH. MV rapidly reacts with $dRfH^{\bullet}$, thus impeding the disproportionation of the $dRfH^{\bullet}$ radical to form the hydroquinone $dRfH_2$ species. In addition, in some cases, viologens improve protein reduction, which is indeed the case for ArsH [$k_2 = 2.9 \times 10^8$ M^{-1} s^{-1} (Table 1)].

In the presence of added quinones, slow kinetics of ArsH reoxidation were obtained in most cases (Figure 6, top inset), with observed rate constant values (k_{SQ}') independent of quinone concentration (Figure 6, bottom, and Table 1), indicating the occurrence of a first-order reduction process. DBMIB and dimethyl-*p*-BQ were, however, very much reactive toward both MV and dRf versus ArsH, thus competing with protein reduction. Under these conditions, it was possible to observe only ArsH reduction (and reoxidation) at very low concentrations of the quinones (<2 μM). Although a concentration dependence study was not possible, relatively fast rates of ArsH oxidation were observed at the low quinone concentrations assayed (Table 1). On the other hand, AQS proved to be unreactive toward $ArsH_{SQ}$ on a time scale of seconds (not shown).

ArsH Deletion Mutants. We have analyzed the growth of both an *arsH* deletion (SARSH) and an *arsR* deletion (SARSR) strain, the latter expressing the *arsBHC* operon constitutively,[6] under oxidative stress generated by the presence of menadione (Figure 7). In all cases, cells were grown both in the absence or presence of arsenite, which acts as an inductor of the expression of the *arsBHC* operon.[6] ArsH confers protection against the addition of menadione under conditions in which this protein is expressed, either in the SARSR strain, in the absence and presence of arsenite, or in the wild type in the presence of arsenite. However, SARSH cells are sensitive to menadione in the presence of arsenite (Figure 7), suggesting that ArsH could play a role in protecting cells under oxidative stress generated by arsenite.

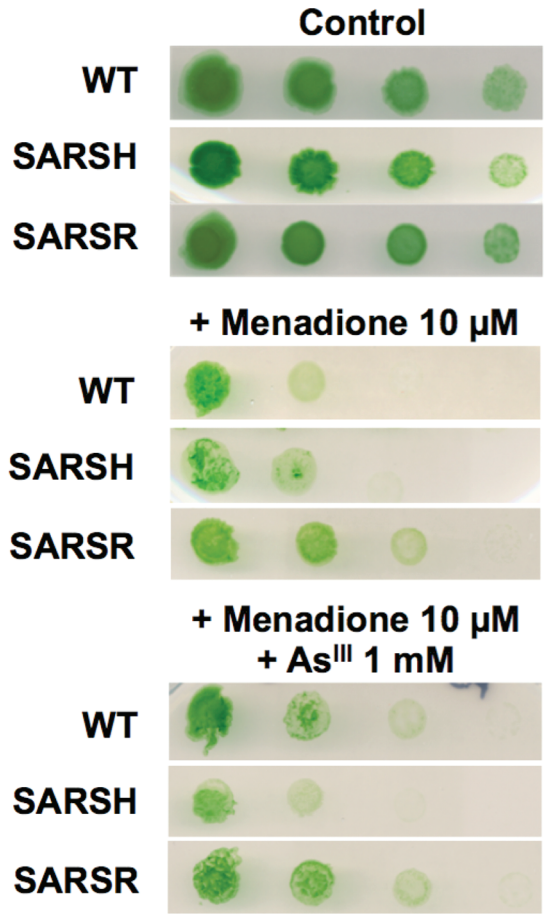

Figure 7. Analysis of the growth of the SARSH strain as compared with the wild-type (WT) and SARSR *Synechocystis* strains. All strains were grown in BG11C liquid medium up to the exponential phase (3 μg of chlorophyll/mL). Then the cells were diluted to a concentration of 1 μg of chlorophyll/mL and finally, by dilution factors of 10, were plated on solid medium supplemented with 10 μM menadione, with or without 1 mM arsenite. Every spot contained initially 5 μL of the corresponding diluted cell culture. The plates were maintained at 30 °C for 5–7 days to visualize the observed growth. Ten-fold dilutions are shown from left to right.

DISCUSSION

Synechocystis ArsH has been successfully expressed in *E. coli* as a FMN-containing protein with typical flavoprotein properties, as

dx.doi.org/10.1021/bi201904p | *Biochemistry* 2012, 51, 1178–1187

are the absorption spectrum and redox potential. The recombinant enzyme seems to form a tetramer in solution (molecular mass of ~108 kDa), in agreement with previous reports of a dimer of dimers for homologous proteins.[10,15,20] ArsH preferentially uses NADPH as an electron donor, and from the stopped-flow kinetics, it can be assumed that the formation of the initial NADPH:$ArsH_{OX}$ charge-transfer complex and the hydride-transfer step can be identified with the first and second phases of the absorbance change, respectively, which include the formation of the catalytically competent complex. With regard to the catalytic relevance of the third slowest phase, it has been previously explained by the formation of a E_{red}:$NADP^+$ charge-transfer complex and the release of $NADP^+$.[30] However, assigning this phase solely to the release of $NADP^+$ after enzyme reduction is not compatible with data for quinone reduction (see below), as the very slow k_3' rate (2 s^{-1}), although measured at a lower temperature, should decrease k_{cat} values for the overall process determined by steady-state experiments (Table 1). Thus, the third phase is not rate-limiting in catalysis. A key observation is that the amplitude of this phase decreases with an increasing NADPH concentration, a fact compatible with the formation of an E_{red}:$NADP^+$ charge-transfer species, but in which NADPH can displace $NADP^+$ as the NADPH concentration increases.[30−34] An alternative explanation is that probably this slowest step observed in the stopped-flow measurements might either alter its rate or disappear in the presence of the acceptor substrate. In any case, the values reported here for the different catalytic steps involving NADPH, i.e., the formation of the initial charge-transfer complex, partner K_A, the NADPH:FMN electron-transfer rate, and NADPH K_m, are in the range of the values previously described for other flavin-dependent enzymes.[30−34]

Bacterial NAD(P)H-dependent flavoproteins have been reported to use FMN, azo dyes, nitro-aromatic compounds, or quinones as substrates.[20] Our kinetic analysis indicates that ArsH is a very efficient NADPH-dependent quinone-reductase, able to reduce quinones with one to three aromatic rings with K_m values as low as 1−2 μM and E_{cat} values as high as 10^7 M^{-1} s^{-1} (Table 1). The higher kinetic efficiencies correspond to quinones with a single ring and methyl groups close to the 1-position keto group (Figure 1). As previously shown in other quinone reductases, quinone affinities and catalytic efficiencies drastically decrease as the number of quinone rings increases (Figure 1 and Table 1),[20] as shown both by stopped-flow data and steady-state activity analysis. The ArsH-catalyzed reduction of quinones follows a ping-pong-type mechanism, in which the NADPH reductant binds first to the active site to deliver electrons and then dissociates to allow the quinone substrate to bind and be reduced, preferentially by a two-electron transfer, resulting in the direct formation of the hydroquinone species of the acceptor. Comparison of the steady-state and transient kinetic results clearly suggests the reductive half-reaction limits the overall reaction; in quinone-reductases, the substrate reduction process has been proposed to occur through two direct hydride-transfer steps, involving the stabilization of the negative charge on the reduced cofactor after $NADP^+$ dissociation.[21,39] In this mechanism, $NADP^+$ can act as an inhibitor, most likely by competing for NADPH binding at the active site, as shown here. However, $ArsH_{HQ}$ is also able to conduct slow one-electron reductions of nonspecific substrates, such as *Cc* or O_2. Thus, although acting as an efficient quinone reductase, the ArsH protein presents biochemical features different from those of other conventional NQO1 quinone reductases.[20] The results obtained with oxygen are of particular interest, as ArsH has been proposed to be a "H_2O_2 generator" on the outside of the cytoplasm, as part of a mechanism of oxidation of arsenite to the less toxic arsenate species.[15,38] *Synechocystis* $ArsH_{HQ}$, however, acts as a quite inefficient oxygen reductant to produce H_2O_2 via superoxide generation, either directly or in a manner mediated by reduced quinones.

The structure of *Synechocystis* ArsH has not yet been determined, but crystal structures of the highly homologous ArsH proteins from *S. meliloti* and *Sh. flexneri* are available in the apo form,[10,15] as well as the structure of a related FMN-reductase holoprotein from *P. aeruginosa*.[27] Figure 8 shows

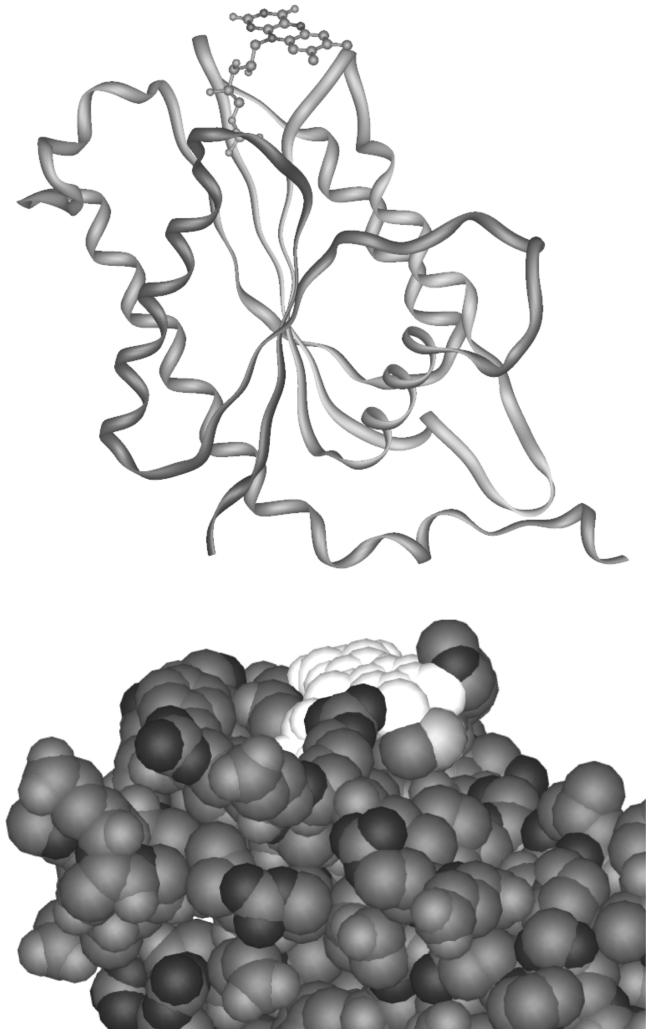

Figure 8. Ribbon structure (top) of the flavodoxin-like catalytic domain of the *Synechocystis* ArsH monomer, as obtained by molecular modeling. The FMN cofactor is shown as balls and sticks. CPK model (bottom) of the ArsH active site. The FMN cofactor is colored white. In both drawings, the orientation of the protein is the same.

ribbon and CPK models of the flavodoxin-like catalytic domain of the *Synechocystis* ArsH monomer, as obtained by molecular modeling. The model shows a FMN cofactor very accessible to the solvent, thus explaining a redox potential value quite similar to that of free FMN, as well as the more positive redox potential of ArsH as compared with flavodoxins and its reactivity with *Cc*. As previously shown for other NAD(P)H-dependent flavoenzymes,[27,39] the FMN is located in a cavity

dx.doi.org/10.1021/bi201904p | *Biochemistry* 2012, 51, 1178−1187

placed in the interface between two monomers (not shown), thus offering an unique place to bind both NADPH and quinones with different sizes and structures.

Whereas many bacterial quinone reductases possess high azoreductase activity, in the case of ArsH this is merely residual. In addition, as compared with other quinone reductases, ArsH exhibits weak inhibition by dicoumarol. These facts can be explained because, although the ArsH flavodoxin-like fold is structurally related to other quinone reductases, the protein is not homologous enough to canonical NQO1 quinone reductases.[20] In the specific case of dicoumarol inhibition, it has been previously proposed that its strong binding to animal quinone reductases can be explained by the hydrophobic interaction with the phenol ring of a tyrosine residue that is absent in *Synechocystis* ArsH.[40] Interestingly, the cyanobacterial ArsH sequence maintains a histidine residue (His-83) very close to the isoalloxazine FMN ring, presumably involved in the stabilization of the negative charge on the flavin cofactor upon $NADP^+$ dissociation.[39]

To establish the mechanism of the ArsH-catalyzed quinone reduction, it is important to consider that flavoenzymes can reduce quinones via one- or two-electron transfers. The former mechanism should involve the generation of flavosemiquinone intermediates in the enzyme cofactor as well as semiquinone substrates. In the case of ArsH, it is not possible to easily detect $ArsH_{SQ}$ formation during quinone reduction, because of the lack of the specific absorbance features of the neutral $ArsH_{SQ}$ species in the 500−700 nm range. In spite of this, the results obtained by using *Cc* and H_2O_2 as reporters support the finding that NADPH-dependent quinone reduction by ArsH follows preferentially a two-electron-transfer process. However, as previously noted, $ArsH_{HQ}$ also supports slow one-electron reactions with substrates other than quinones. In addition, by using low-potential one-electron probes, such as dRf or viologens, it is possible to generate a stable $ArsH_{SQ}$ anionic species, as demonstrated by the laser-induced differential spectrum. Similar processes of semiquinone formation have been previously reported for glutathione reductase, a two-electron-transfer NADPH:flavin-disulfide enzyme, and animal NADPH:quinone reductase.[41,42] Thus, even though the formation of $ArsH_{SQ}$ could be considered a nonphysiological process in a NADPH-dependent enzyme, the question about the ability of $ArsH_{SQ}$ to form one-electron-reduced quinones arises. However, our data suggest that the reactivity of $ArsH_{SQ}$ toward oxidized quinones is diminished as compared with that of the $ArsH_{HQ}$ form. For most of the quinones assayed, $ArsH_{HQ}$ oxidation occurs within the dead time of the stopped-flow instrument ($k_{obs} \geq 200\ s^{-1}$, and is much faster in any case than $ArsH_{SQ}$ oxidation, measured by laser-flash spectroscopy (Table 1). The only exception is dimethyl-*p*-BQ, for which rapid reactions are observed with the two reduced species of ArsH.

In vivo experiments with *ars* mutants showed however that, although ArsH has no essential role in arsenic resistance,[6] it can play a role in protecting *Synechocystis* against oxidative stress. It has been suggested that one of the main side effects of arsenic compounds is the generation of ROS, which is mediated by the binding of arsenite to sulfur side chains of proteins, thus promoting the inhibition of its function

Finally, although ArsH has no direct role in the protection against oxidative compounds, it could help to cope with damage generated by arsenite, acting by reducing semiquinone radicals or oxidized quinones when the photosynthetic and/or respiratory chains are compromised.

■ ASSOCIATED CONTENT

Supporting Information

Protein sequence alignements of *Synechocystis* ArsH with other ArsH proteins (Figure S1) and plant quinone-reductases (Figure S2). This material is available free of charge via the Internet at http://pubs.acs.org.

■ AUTHOR INFORMATION

Corresponding Author

*Instituto de Bioquímica Vegetal y Fotosíntesis, Centro de Investigaciones Científicas Isla de la Cartuja, CSIC and Universidad de Sevilla, Américo Vespucio 49, 41092 Seville, Spain. Telephone: 34-954-489-515. Fax: 34-954-460-065. E-mail: jnavarro@ibvf.csic.es.

Funding

This work was supported by the Andalusian Government (PAIDI BIO-022), cofinanced with FEDER (to J.A.N.), and Grant BFU2010-15708, cofinanced by FEDER, to F.J.F. from the Ministerio de Ciencia e Innovación.

Notes

The authors declare no competing financial interest.

■ ACKNOWLEDGMENTS

We thank Prof. Gordon Tollin for providing us with deazariboflavin.

■ ABBREVIATIONS

AQS, anthraquinone-2-sulfonate; $ArsH_{OX}$, $ArsH_{SQ}$, and $ArsH_{HQ}$, ArsH in its oxidized, semiquinone, and hydroquinone forms, respectively; *Cc*, horse mitochondrial cytocrome *c*; DBMIB, dibromothymoquinone; DCPIP, dichlorophenolindophenol; dRf and $dRfH^{\bullet}$, 5-deazariboflavin and its reduced radical, respectively; dimethyl-*p*-BQ, 2,5-dimethyl-*p*-benzoquinone; E_{cat}, catalytic efficiency (k_{cat}/K_m); FAD, flavin adenine dinucleotide; FMN, flavin mononucleotide; k_{cat}, catalytic constant; k_{obs}, observed pseudo-first-order rate constant; K_A, association constant; k_2' and k_3', apparent first-order electron-transfer rate constants for the second and third phases, respectively, of reduction of ArsH by NADPH; k_2, second-order rate constant for a bimolecular reaction; k_{SQ}' and k_{HQ}', observed first-order electron-transfer rate constants for oxidation of $ArsH_{SQ}$ and $ArsH_{HQ}$, respectively, by quinones; MV, methyl-viologen; 2-OH-1,4-NQ, 2-hydroxy-1,4-naphthoquinone; $O_2^{\bullet-}$, superoxide radical.

■ REFERENCES

(1) van Berkel, W. J. H. (2008) Chemistry of Flavoenzymes. In *Wiley Encyclopedia of Chemical Biology (Tadhg Begley, Chair)*, pp 1−11. John Wiley & Sons, Inc., New York.

(2) Nordstrom, D. K. (2002) Public health. Worldwide occurrences of arsenic in ground water. *Science 296*, 2143−2145.

(3) Shi, H., Shi, X., and Liu, K. J. (2004) Oxidative mechanism of arsenic toxicity and carcinogenesis. *Mol. Cell. Biochem. 255*, 67−78.

(4) Rosen, B. P. (1999) Families of arsenic transporters. *Trends Microbiol. 7*, 207−212.

(5) Rosen, B. P. (2002) Biochemistry of arsenic detoxification. *FEBS Lett. 529*, 86−92.

(6) López-Maury, L., Florencio, F. J., and Reyes, J. C. (2003) Arsenic sensing and resistance system in the cyanobacterium *Synechocystis* sp. strain PCC 6803. *J. Bacteriol. 185*, 5363−5371.

(7) Carlin, A., Shi, W., Dey, S., and Rosen, B. P. (1995) The *ars* operon of *Escherichia coli* confers arsenical and antimonial resistance. *J. Bacteriol. 177*, 981−986.

(8) Neyt, C., Iriarte, M., Thi, V. H., and Cornelis, G. R. (1997) Virulence and arsenic resistance in Yersiniae. *J. Bacteriol. 179*, 612−619.
(9) Butcher, B. G., Deane, S. M., and Rawlings, D. E. (2000) The chromosomal arsenic resistance genes of *Thiobacillus ferrooxidans* have an unusual arrangement and confer increased arsenic and antimony resistance to *Escherichia coli*. *Appl. Environ. Microbiol. 66*, 1826−1833.
(10) Vorontsov, I. I., Minasov, G., Brunzelle, J. S., Shuvalova, L., Kiryukhina, O., Collart, F. R., and Anderson, W. F. (2007) Crystal structure of an *apo* form of *Shigella flexneri* ArsH protein with an NADPH-dependent FMN reductase activity. *Protein Sci. 16*, 2483−2490.
(11) López-Maury, L., Sánchez-Riego, A. M., Reyes, J. C., and Florencio, F. J. (2009) The glutathione/glutaredoxin system is essential for arsenate reduction in *Synechocystis* sp. strain PCC 6803. *J. Bacteriol. 191*, 3534−3543.
(12) Li, R., Haile, J. D., and Kennelly, P. J. (2003) An arsenate reductase from *Synechocystis* sp. strain PCC 6803 exhibits a novel combination of catalytic characteristics. *J. Bacteriol. 185*, 6780−6789.
(13) Ryan, D., and Colleran, E. (2002) Arsenical resistance in the IncHI2 plasmids. *Plasmid 47*, 234−240.
(14) Yang, H. C., Cheng, J., Finan, T. M., Rosen, B. P., and Bhattacharjee, H. (2005) Novel pathway for arsenic detoxification in the legume symbiont *Sinorhizobium meliloti*. *J. Bacteriol. 187*, 6991−6997.
(15) Ye, J., Yang, H. C., Rosen, B. P., and Bhattacharjee, H. (2007) Crystal structure of the flavoprotein ArsH from *Sinorhizobium meliloti*. *FEBS Lett. 581*, 3996−4000.
(16) Mayhew, S. G., and Massey, V. (1969) Purification and characterization of flavodoxin from *Peptostreptococcus elsdenii*. *J. Biol. Chem. 244*, 794−802.
(17) Light, D. R., Walsh, C., and Marletta, M. A. (1980) Analytical and preparative high-performance liquid chromatography separation of flavin and flavin analog coenzymes. *Anal. Biochem. 109*, 87−93.
(18) Rodríguez-Roldán, V., García-Heredia, J. M., Navarro, J. A., Hervás, M., De la Cerda, B., Molina-Heredia, F. P., and de la Rosa, M. A. (2006) A comparative kinetic analysis of the reactivity of plant, horse and human respiratory cytochrome *c* towards cytochrome *c* oxidase. *Biochem. Biophys. Res. Commun. 336*, 1108−1113.
(19) Bin, Y., Jiti, Z., Jing, W., Cuihong, D., Hongman, H., Zhiyong, S., and Yongming, B. (2004) Expression and characteristics of the gene encoding azoreductase from *Rhodobacter sphaeroides* AS1.1737. *FEMS Microbiol. Lett. 236*, 129−136.
(20) Deller, S., Macheroux, P., and Sollner, S. (2008) Flavin-dependent quinone reductases. *Cell. Mol. Life Sci. 65*, 141−160.
(21) Gonzalez, C. F., Ackerley, D. F., Lynch, S. V., and Matin, A. (2005) ChrR, a soluble quinone reductase of *Pseudomonas putida* that defends against H_2O_2. *J. Biol. Chem. 280*, 22590−22595.
(22) Fontes, A. G., De la Rosa, F. F., and Gómez-Moreno, C. (1981) Continuous photochemical production of hydrogen peroxide catalyzed by flavins. *Photobiochem. Photobiophys. 2*, 355−364.
(23) Tollin, G. (1995) Use of flavin photochemistry to probe intraprotein and interprotein electron transfer mechanisms. *J. Bioenerg. Biomembr. 27*, 303−309.
(24) Navarro, J. A., Hervás, M., Pueyo, J. J., Medina, M., Gómez-Moreno, C., de la Rosa, M. A., and Tollin, G. (1994) Laser flash-induced photoreduction of photosynthetic ferredoxins and flavodoxin by 5-deazariboflavin and by a viologen analogue. *Photochem. Photobiol. 60*, 231−236.
(25) Rodríguez-Roldán, V., García-Heredia, J. M., Navarro, J. A., de la Rosa, M. A., and Hervás, M. (2008) Effect of nitration on the physico-chemical and kinetic features of wild-type and mono-tyrosine mutants of human respiratory cytochrome. *c. Biochemistry 47*, 12371−12379.
(26) Meyer, T. E., Zhao, Z. G., Cusanovich, M. A., and Tollin, G. (1993) Transient kinetics of electron transfer from a variety of c-type cytochromes to plastocyanin. *Biochemistry 32*, 4552−4559.
(27) Agarwal, R., Bonanno, J. B., Burley, S. K., and Swaminathan, S. (2006) Structure determination of an FMN reductase from *Pseudomonas aeruginosa* PA01 using sulfur anomalous signal. *Acta Crystallogr. D62*, 383−391.
(28) Deller, S., Sollner, S., Trenker-El-Toukhy, R., Jelesarov, I., Gübitz, G. M., and Macheroux, P. (2006) Characterization of a thermostable NADPH:FMN oxidoreductase from the mesophilic bacterium *Bacillus subtilis*. *Biochemistry 45*, 7083−7091.
(29) Edmondson, D. E., and Tollin, G. (1983) Semiquinone formation in flavo- and metalloflavoproteins. *Top. Curr. Chem. 108*, 109−138.
(30) Massey, V., Matthews, R. G., Foust, G. P., Howell, L. G., Williams, C. H., Zanetti, G., and Ronchi, S. (1970) A new intermediate in TPNH-linked flavoproteins. In *Pyridine Nucleotide-Dependent Dehydrogenases* (Sund, H., Ed.) pp 393−411, Springer-Verlag, Berlin.
(31) Gutierrez, A., Lian, L.-Y., Wolf, C. R., Scrutton, N. S., and Roberts, G. C. K. (2001) Stopped-flow kinetic studies of flavin reduction in human cytochrome P450 reductase and its component domains. *Biochemistry 40*, 1964−1975.
(32) Knight, K., and Scrutton, N. S. (2002) Stopped-flow kinetic studies of electron transfer in the reductase domain of neuronal nitric oxide synthase: Re-evaluation of the kinetic mechanism reveals new enzyme intermediates and variation with cytochrome P450 reductase. *Biochem. J. 367*, 19−30.
(33) Williams, C. H., Jr. (1992) Lipoamide dehydrogenase, glutathione reductase, thioredoxin reductase, and mercuric ion reductase: A family of flavoenzyme transhydrogenases. In *Chemistry and Biochemistry of Flavoenzymes* (Müller, F., Ed.) *Vol. 3*, pp 121−211, CRC Press, Boca Raton, FL.
(34) Brett, W. L., and Williams, C. H. Jr. (1997) Reductive half-reaction of thioredoxin reductase from *Escherichia coli*. *Biochemistry 36*, 9464−9477.
(35) Lennon, B. W., Williams, C. H. Jr., and Ludwig, M. L. (2000) Twists in catalysis: Alternating conformations of *Escherichia coli* thioredoxin reductase. *Science 289*, 1190−1194.
(36) Lind, C., Hochstein, P., and Ernster, L. (1982) DT-diaphorase as a quinone reductase: A cellular control device against semiquinone and superoxide radical formation. *Arch. Biochem. Biophys. 216*, 178−185.
(37) Ackerley, D. F., Gonzalez, C. F., Park, C. H., Blake, R. II, Keyhan, M., and Matin, A. (2004) Chromate-reducing properties of soluble flavoproteins from *Pseudomonas putida* and *Escherichia coli*. *Appl. Environ. Microbiol. 70*, 873−882.
(38) Wu, X.-L., Miao, B., Han, J., Hu, Q., Zeng, J., Liu, Y.-D., and Qiu, G.-Z. (2010) Purification and enzymatic properties of arsenic resistance protein ArsH from heterogeneous expression in *E. coli* BL21. *Trans. Nonferrous Met. Soc. China 20*, 1987−1992.
(39) Bianchet, M. A., Faig, M., and Amzel, L. M. (2004) Structure and mechanism of NAD[P]H:quinone acceptor oxidoreductases (NQO). *Methods Enzymol. 382*, 144−174.
(40) Chen, S., Wu, K., Zhang, D., Sherman, M., Knox, R., and Yang, C. S. (1999) Molecular characterization of binding of substrates and inhibitors to DT-diaphorase: Combined approach involving site-directed mutagenesis, inhibitor-binding analysis, and computer modeling. *Mol. Pharmacol. 56*, 272−278.
(41) Navarro, J. A., Gleason, F. K., Cusanovich, M. A., Fuchs, J. A., Meyer, T. E., and Tollin, G. (1991) Kinetics of electron transfer from thioredoxin reductase to thioredoxin. *Biochemistry 30*, 2192−2195.
(42) Tedeschi, G., Chen, S., and Massey, V. (1995) DT-diaphorase. Redox potential, steady-state and rapid reaction studies. *J. Biol. Chem. 270*, 1198−1204.